

Design Optimization and Performance Studies of an Adult Scale Viscous Impeller Pump for Powered Fontan in an Idealized Total Cavopulmonary Connection

JEFFREY R. KENNINGTON,¹ STEVEN H. FRANKEL,¹ JUN CHEN,¹ STEVEN C. KOENIG,^{2,3}
MICHAEL A. SOBIESKI,^{2,3} GURUPRASAD A. GIRIDHARAN,² and MARK D. RODEFELD⁴

¹School of Mechanical Engineering, Purdue University, 500 Allison Road, West Lafayette, IN 47907, USA; ²Department of Bioengineering, University of Louisville, Louisville, KY 40292, USA; ³Department of Surgery, University of Louisville, Louisville, KY 40292, USA; and ⁴Department of Surgery, Indiana University School of Medicine, Indianapolis, IN 46202, USA

(Received 9 November 2010; accepted 28 July 2011)

Associate Editor Keefe B. Manning oversaw the review of this article.

Abstract—Numerical and experimental studies are carried out to assess the hydraulic and hemodynamic performance and the biocompatibility of a viscous impeller pump (VIP) for cavopulmonary assist in patients with a univentricular Fontan circulation. Computational fluid dynamics (CFD) predictions of impeller performance are shown to be in very good agreement with measured pressure-flow data obtained in a Fontan mock-circulation system. Additional CFD and experimental design studies intending to balance pump performance and biocompatibility with the manufacturability limitations of a percutaneous expandable impeller are also reported. The numerical models and experimental studies confirm excellent performance of the VIP with augmentation of Fontan pressure up to 35 mmHg for flow rates up to 4.5 L/min and operational speeds no higher than 5000 RPM. Scalar stress predictions on the VIP surface and laboratory hemolysis measurements both demonstrate very low hemolysis potential. The impeller designs reported offer ideal performance and can meet manufacturing tolerances of a flexible, catheter-based percutaneous expandable rotary pump.

Keywords—Powered Fontan, Assist device, Total cavopulmonary connection, Hemolysis, Hypoplastic.

INTRODUCTION

Single ventricle heart disease is the leading cause of death from any birth defect in the first year of life.⁵ The most common of these defects is hypoplastic left heart syndrome, in which the only functional ventricle is a

morphologically right ventricle. The current procedure to palliate this defect is to bypass the right-sided circulation completely and rely upon the single functional ventricle to supply motive force to the systemic and pulmonary circulations in series. This reparative process, known as staged Fontan palliation, consists of three sequential surgeries: the Norwood procedure, the hemi-Fontan or Glenn procedure, and the completion Fontan procedure, as shown in Fig. 1. The final reconfigured blood vessel geometry is known as the total cavopulmonary connection (TCPC), in which blood flows passively from both vena cavae into the pulmonary arteries to perfuse the lungs. The systemic and pulmonary circulations thus depend upon the single functional ventricle to produce the required pressure for the entire circulatory system. Even though the existing staged palliative approach to yield Fontan physiology results in significant improvement in survival, it remains highly problematic with only a 50–70% survival rate through all three surgeries.¹² Among survivors, serious long-term functional complications are common. Many are attributable to elevated systemic venous pressure and suboptimal ventricular filling which exist after completion of Fontan repair. These complications are due in some respect to energy losses and irregular flow and mixing features in the TCPC. In this anatomy, there are two confined impinging jets (the superior and inferior vena cava (SVC/IVC)) which exhaust into two confined, nearly perpendicular, outlets associated with the left and right pulmonary arteries (LPA/RPA). It is generally accepted that minimization of energy loss at the level of the TCPC junction would improve hemodynamic status and quality of life.²⁰

Address correspondence to Steven H. Frankel, School of Mechanical Engineering, Purdue University, 500 Allison Road, West Lafayette, IN 47907, USA. Electronic mail: jkenning@purdue.edu, frankel@purdue.edu

To address this problem, detailed and elegant studies have been performed to investigate the flow dynamics in the four-way TCPC junction using either idealized or patient-specific geometries and *in vitro* models (see Dasi *et al.*⁴ and references cited therein). There are currently two principal areas of focus to improve hemodynamic characteristics in the Fontan venous pathway. The first is passive flow control, which aims to reduce the dissipative flow energy losses in Fontan physiology through optimized surgical reconstruction of the TCPC at the time of, or subsequent to, Fontan palliation. Two recent examples include splitting of one or both inlets. A Y-shaped modification has been proposed to split the IVC flow toward the right and left pulmonary arteries.¹¹ The IVC is a preferential therapeutic target over the SVC because the majority of systemic venous return arises from the IVC distribution in adults (70%) and the majority of medical problems of late Fontan failure

stem from this distribution.¹¹ In another variation, a flow 4-way splitting device (Optiflo) has been proposed to split both SVC and IVC flow into the pulmonary arteries.¹⁷ Passive flow optimization holds promise to improve flow in the TCPC and reduce energy losses. However, these modifications may be difficult to implement surgically with concern for thrombus formation and injury to adjacent anatomic structures (e.g., phrenic nerve). Whether clinical benefit outweighs surgical risk remains to be determined. It is also important to note that as the patient matures with somatic growth the relative distribution of IVC and SVC flow will change and the growth potential of these variations may limit application in childhood.

A second method to improve Fontan circulatory status, and the focus of our investigative effort, is active flow augmentation at the level of the TCPC through development of some form of mechanical cavopulmonary assist device.¹⁵ In Fontan physiology, there is a relative increase in systemic venous pressure and decrease in pulmonary arterial pressure (Fontan paradox).⁴ A partial assist device in the TCPC pathway which can provide 2–5 mmHg pressure augmentation will simultaneously reduce systemic venous pressure and increase pulmonary arterial pressure to restore conditions more closely resembling a more stable two ventricle circulation. Prior implementations of mechanical cavopulmonary assist have been limited to experimental studies, and have focused on the use of microaxial pumps.¹⁴ In our experience, however, we have found that achieving the desired 4-way flow augmentation in a pattern characteristic of the TCPC junction with existing microaxial pumps is problematic. The limitations of unidirectional microaxial flow devices include: (1) a need for 2 devices to satisfactorily augment the double inlet, double outlet flow 4-way pattern characteristic of the TCPC, increasing the complexity of implantation and explantation, and risk of failure; (2) microaxial pumps are obstructive, which limits the ability to wean support to no net contribution to Fontan flow, and may be catastrophic in the event of pump failure; (3) microaxial pumps have an inherently high risk of inlet suction due to high rotational speed; (4) if 2 devices are used, both must provide balanced flows to prevent back pressure elevation in the opposing venous territory. Use of a single device in the IVC territory will induce back pressure elevation in the SVC. To avoid these limitations, surgical modification of the existing Fontan junction to a Y-shaped 3-way junction has been proposed.⁹ While this approach may enable Fontan support using a single unidirectional microaxial pump in the common outflow limb, it would require an additional major surgical procedure with cardiopulmonary bypass to reconstruct the Fontan cavopulmonary junction. Further, implantation of a

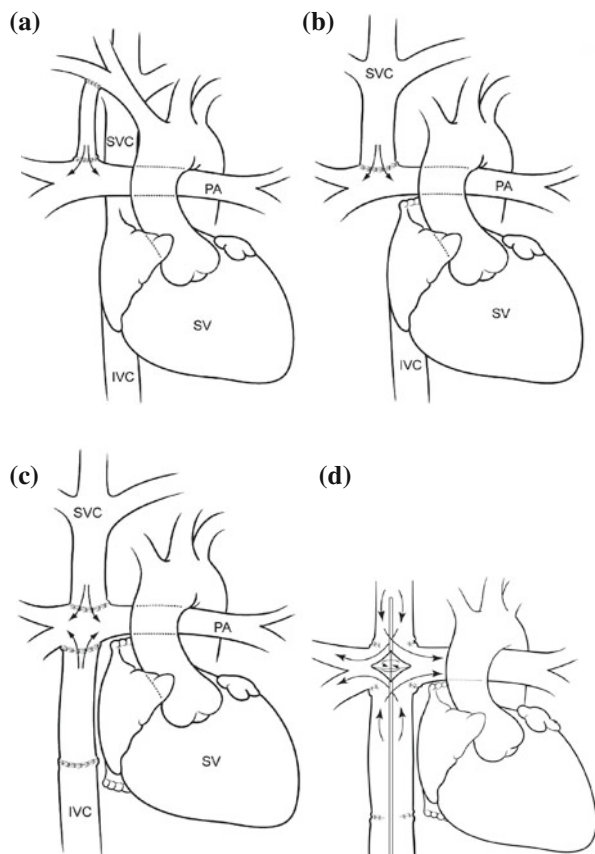


FIGURE 1. Staged surgical repair of single ventricle. (a) Stage 1 (Norwood repair): Blood flow to lungs is derived from systemic-to-pulmonary artery shunt. (b) Stage 2 (Hemi-Fontan repair): The SVC is connected to pulmonary artery as only source of pulmonary blood flow. IVC flow is ejected back out to body. (c) Stage 3 (Fontan completion): IVC flow is diverted to the pulmonary artery to form a TCPC (SV, single ventricle; PA, pulmonary artery). (d) Powered completion using a Cavopulmonary Assist Device (Powered Fontan).

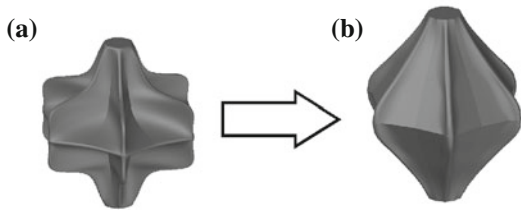


FIGURE 2. Successive VIP iterations. (a) Design 1 and (b) Design 2.

microaxial pump in a 3-way junction does not resolve the problems of obstruction, pump failure, and weaning of support.

We have identified a cavopulmonary assist concept which requires one pump and will address 4-directional flow.¹⁵ An expandable viscous impeller pump (VIP), based on the von Kármán viscous pump principle, appears to satisfactorily address these problems. The application of the VIP to the Fontan is defined here as Powered Fontan. The VIP, deployed at the intersection of an in vitro TCPC model, not only stabilizes (static device) but also augments (rotational device) the existing four-way TCPC flow pattern.²¹ It is not obstructive to flow and can be placed percutaneously.

The objectives of the present study are twofold. First, CFD is used to converge on a VIP design which merges pump performance specifications with the manufacturability constraints of a percutaneous expandable rotary platform. Second, CFD predictions are compared to measured flow-pressure data to both validate the numerical models and to assess the hemodynamic performance and biocompatibility of VIP design. By comparing the CFD design with an early scale prototype morphology, we have characterized an optimal pre-clinical design. The hydraulic performance and biocompatibility of the two designs are examined using the physiologic parameters of an idealized TCPC. The VIP designs presented in this study represent a progression in optimization from an early preliminary design (Design 1) to an optimized design (Design 2) which meets hydraulic, shear stress, thrombogenicity, and hemolysis specifications, and is manufacturable using appropriate materials which will be used in a clinical device (Fig. 2).

NUMERICAL SIMULATION APPROACH

The Fluent (ANSYS Inc., Cannonsburg, PA) CFD software was used to predict TCPC hemodynamics induced by the VIP. The Unsteady Reynolds-Averaged Navier–Stokes (URANS) approach was employed to compute the ensemble-averaged velocity field, $\bar{u}_i(\mathbf{x}, t)$, and pressure field, $\bar{p}(\mathbf{x}, t)$. Due to the unsteady nature

TABLE 1. Design specifications of blood pump for adult single ventricle patient based on clinically reported data.

Design	Measurement
Volumetric flow (LPM)	0.5–4.4
VIP rotational speed (RPM)	1000–5000
Vena cava diameter (mm)	22
Maximum impeller diameter (mm)	19
PA diameter (mm)	18

of the flow near the impeller, a laminar model was unable to converge and a turbulence model was required. The realizable $k - \epsilon$ model was therefore used for turbulence closure. The computational domain was constructed using the geometry of an idealized TCPC at adult-scale. The fluid medium was assigned a physiologic density of 1060 kg/m^3 and viscosity of $3.5 \times 10^{-3} \text{ Pa} \cdot \text{s}$, corresponding to an estimated hematocrit of 33%; both were assumed to be constant. Equal SVC/IVC inlet flow rates and a weighted 50:50 outflow RPA/LPA split was enforced in the simulation. Geometric details, flow rates, and pump rotation rates are specified in Table 1.

The computational domain was generated using Solid Edge to create the solid model and Gambit (preprocessor for Fluent) to generate the mesh. The meshes contain two million tetrahedral elements with a concentration near the center of the TCPC junction and around the VIP. The pump motion was modeled using the sliding mesh method available within Fluent.⁷ This was accomplished by creating a cylindrical fluid domain surrounding the VIP inside of the TCPC geometry, which was then rotated at prescribed rates for the desired RPM.

Hemolysis Testing

The Pressure Implicit with Splitting of Operators algorithm was used for time advancement within Fluent with pressure interpolation using the standard formulation.⁷ The transient formulations used a second-order implicit scheme. Second-order upwind was used for spatial discretizations. Standard wall functions were applied near the solid surfaces of the TCPC and VIP surface. A turbulent length scale of 22 mm and a 3% turbulent intensity were specified on the inlets. The exact values specified had negligible effect on simulation results. Mesh independence was established by refining the mesh until the results varied by less than 5%. The convergence criterion was set to 10^{-4} . Acceptable aspect ratios of the elements were such that no negative volumes exist within the mesh. Different turbulence models were also tested and the realizable $k - \epsilon$ model was employed as it yields the best agreement with experimental results. VIP designs were

tested with focus on optimizing hydraulic performance within fabrication material constraints.

To quantify the damage potential on red blood cells, the scalar stress of Bludszweit³ was used:

$$\sigma_{\text{scalar}} = \sqrt{\frac{1}{6} \sum (\sigma_{ii} - \sigma_{jj})(\sigma_{ii} - \sigma_{jj}) + \sum \sigma_{ij}\sigma_{ij}} \quad (1)$$

where the stress tensor σ_{ij} is composed of a viscous stress (mean) portion τ_{ij} and Reynolds stress portion R_{ij} :

$$\sigma_{ij} = \tau_{ij} + R_{ij} = \mu \left(\frac{\partial \bar{u}_i}{\partial x_j} + \frac{\partial \bar{u}_j}{\partial x_i} \right) + \rho \overline{u'_i u'_j}. \quad (2)$$

Here μ is the dynamic viscosity. u'_i is velocity fluctuation $u'_i(\mathbf{x}, t) = u_i(\mathbf{x}, t) - \bar{u}_i(\mathbf{x}, t)$. The CFD output was then used to calculate the scalar stress.

EXPERIMENTAL APPROACH

Hydraulic Performance

Hydraulic performance studies of VIP Design 1 were carried out using a previously validated mock circulation system^{6,10,13} modified to simulate Fontan physiology. The system consists of a single ventricle, aorta, arterial compliance, systemic vascular resistance, venous compliance, Fontan junction with cavopulmonary assist device and pulmonary resistance and compliance elements. An idealized model of a total cavopulmonary connection was constructed using 3D printing identical to the CFD domain. Bi-conical impellers specified at 19 mm diameter, 6 surface vanes, 0.5–3 mm vane height were designed using Solid Edge CAD software (Siemens PLM Software, Plano, TX), and were fabricated using stereolithography. High fidelity pressure catheters (Millar Instruments, TX) and flow probes (Transonics, NY) were used to measure pressure and flow 10 cm from the center of the TCPC junction. This is a reasonable distance to gauge the upstream and downstream effects of the pump without obfuscation by potential local turbulence effect, which may exist in proximity to the pump. The VIP was operated at rotational speeds of 1000, 2000, 3000, 4000, and 5000 RPM against 5 different resistance values at each speed. Steady-state pressure and flow values were recorded for each operational condition. Hemodynamic pressure and flow data were signal conditioned and analog-to-digital converted at a sampling rate of 400 Hz and stored for digital analysis using a clinically approved Good Laboratory Practice compliant data acquisition system. An average value was used across the SVC/IVC and LPA/RPA over time. The pressure head developed across the VIP was

plotted against pump flow (H–Q curve) to characterize hydraulic performance.

Device Hemolysis

Blood loop studies were conducted to quantify hemolysis caused by the cavopulmonary assist device for early Design 1, which had the most aggressive surface vane structure, and, thus, the highest potential for hemolysis (Fig. 3). Fresh whole bovine blood (drawn less than 48 h) was used. Blood was heparinized to activated clotting time >300 s (Kaolin tubes), and hematocrit adjusted to $28 \pm 2\%$ with plasma buffer solution (Plasmalyte). The impeller was run at its maximum operational speed against a pump pressure head of 15 mmHg. Total blood volume in the *in vitro* loop was 1 L. *In vitro* blood damage was assessed by measuring plasma free hemoglobin (pfHb), hematocrit, red blood cell, white blood cell, and platelet counts before device operation (baseline) and every hour of device operation over a 6 h period. pfHb was quantified using a Plasma Photometer (HemoCue, Mission Viejo, CA) with paired samples taken at each time point calculated and averaged. Platelet count and hematocrit were measured using CDC Mascot (CDC Technologies, Oxford, CT). The hemolysis study parameters and protocol (duration, blood, blood volume, hematocrit, activated clotting time, temperature, frequency of measurement) were in compliance with U.S. Food and Drug Administration (FDA) guidelines for 510(k) submission and American Society of Testing and Materials (ASTM) standards.

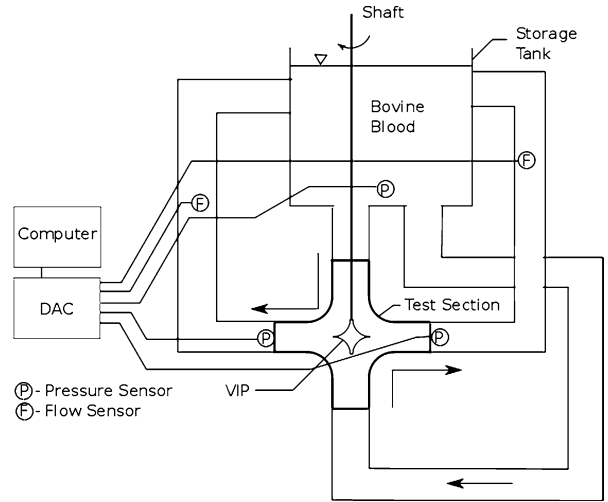


FIGURE 3. *In vitro* blood loop for hemolysis testing.

RESULTS

Model Validation and VIP Performance

Comparison of CFD predictions and mock-loop measurements are shown in Fig. 4. The computational data has an average error of 0.78 mmHg for Design 1 and 1.78 mmHg for Design 2 at 5,000 RPM. The relatively flat pressure-flow (H-Q) curves suggest stable performance of the device over the operational range. Gross cavitation was observed at 10000 RPM for Design 1 and was not observed in Design 2 at 12000 RPM (max specified performance). The rotational speed at which cavitation was observed is well beyond the expected operational range of the device (0–7000 RPM).

Hemolysis Testing

Hemolysis tests using the Design 1 VIP design resulted in a Normalized Index of Hemolysis of 0.07 g/100L, correlating to the acceptable scalar stress shown in Fig. 5a. pfHb at the end of the 6-h test period was

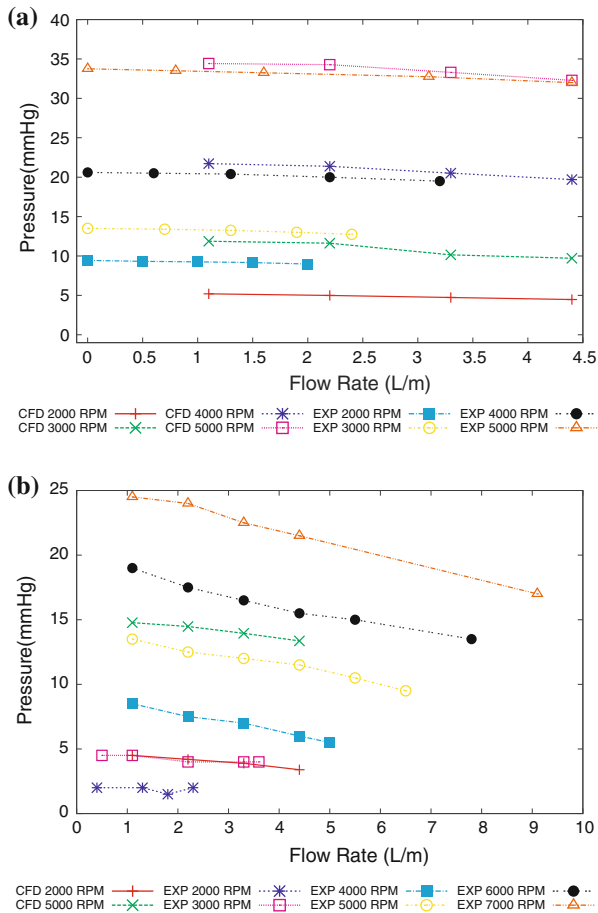


FIGURE 4. CFD and experimental H-Q results. (a) Design 1 and (b) Design 2.

70 mg/dL (average hemolysis rate = 11.4 mg/dL/h, peak hemolysis rate = 20 mg/dL/h). Hematocrit, red cell, white cell, and platelet counts over the 6-h period did not vary significantly from baseline. CFD results predicted a scalar stress (and thus a predicted hemolysis) for Design 2 that is 43% less than Design 1 (Fig. 5). Values of 250 Pa are shown to allow for residence times up to 2 min.¹

Importantly, the removal of damaged red blood cells from the circulation by the liver leads to lower pfHb values clinically. Thus, pfHb values obtained in the hemolysis test loop may be significantly higher than compared to *in vivo* pfHb findings. A pfHb of 70 mg/dL after a 6 h test period for the prototype VIP compares favorably to hemolysis profiles of other clinically approved blood pumps (ventricular assist devices) where pfHb values of 80–250 mg/dL have been reported after 6 h hemolysis testing.^{16,18,19}

Design Studies

The VIP is envisioned to be delivered using a catheter-based percutaneous expandable rotary platform. Hence, design-limited hydraulic performance and hemolysis potential must account for the material and manufacturability constraints for an expandable pump head.

To address this issue, we modified the heavily vaned Design 1 through an iterative optimization process to result in Design 2. The target pressure rise for VIP hydraulic performance was specified at 15 mmHg while limiting a maximum scalar stress to 300 Pa.^{2,8} This higher pressure range may be required to perfuse vasoreactive lungs or patients with pulmonary hypertension, and is safely above the optimal range of 6–8 mmHg pressure necessary for adolescent and adult support as determined in animal studies.¹⁴ Because the heavily vaned Design 1 VIP exceeded the specified pressure range, surface vane structure was subsequently reduced. In this transition, low scalar stress and pressure rise to the target hydraulic performance was maintained, while converging the design to match an early manufactured expanding prototype.¹⁵

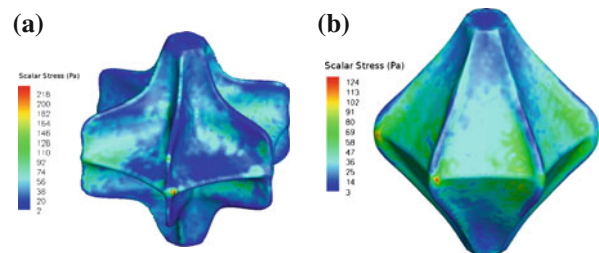


FIGURE 5. Scalar stress on VIP surfaces. (a) Design 1: 5000 RPM 4.4 L/min and (b) Design 2: 5000 RPM 4.4 L/min.

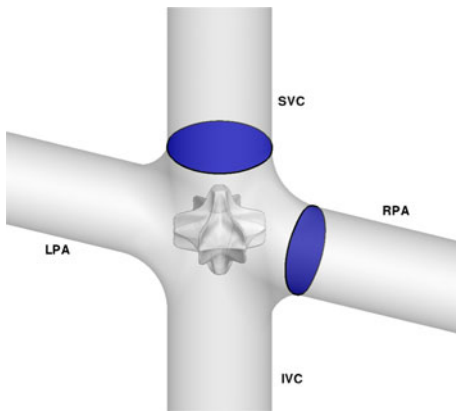


FIGURE 6. Location of cross-section of flow pattern data.

In addition to performance, the pre-pump and post-pump flow fields are important to the assessment of pump-induced hemodynamic losses and thrombosis potential. The velocity profiles and planar velocity vectors are shown at sites illustrated in Fig. 6. The velocity magnitude profiles, from the RANS results, are taken at the SVC and RPA cross-sections located 2.5 cm from the center of the TCPC junction. Rotation rates shown in Fig. 7 were those that had the largest influence on both magnitude and flow pattern. Higher rotation rates resulted in higher velocity magnitudes, scalar stress, and rotation rates of inlet flow. Rotation speeds less than 3,000 RPM are different, as inflow rotation does not dominate the flow pattern. Design 2 flows are more evenly distributed in comparison to Design 1 (Figs. 7d, 7e), presumably as a function of reduced surface vane structure.

VIP induced pre-rotation was noted in the inflow region of the VIP but no areas of stagnation or recirculation were observed. From the RPA cross-section, it can be seen that outflow impacts the pulmonary arterial wall. While this may be initially concerning, it is clinically analogous to the current method in the Norwood procedure of using a systemic-to-pulmonary arterial shunt (a perpendicular stent) where flow from the high pressure systemic arterial circulation impacts the pulmonary arterial wall directly opposite the site of shunt insertion. Clinically, this impact is not associated with thrombus formation or pulmonary arterial wall damage.

CONCLUSION

Hemodynamic performance and biocompatibility of a viscous impeller pump for cavopulmonary assist of the univentricular Fontan circulation was assessed using CFD validated with mock loop H-Q measurements

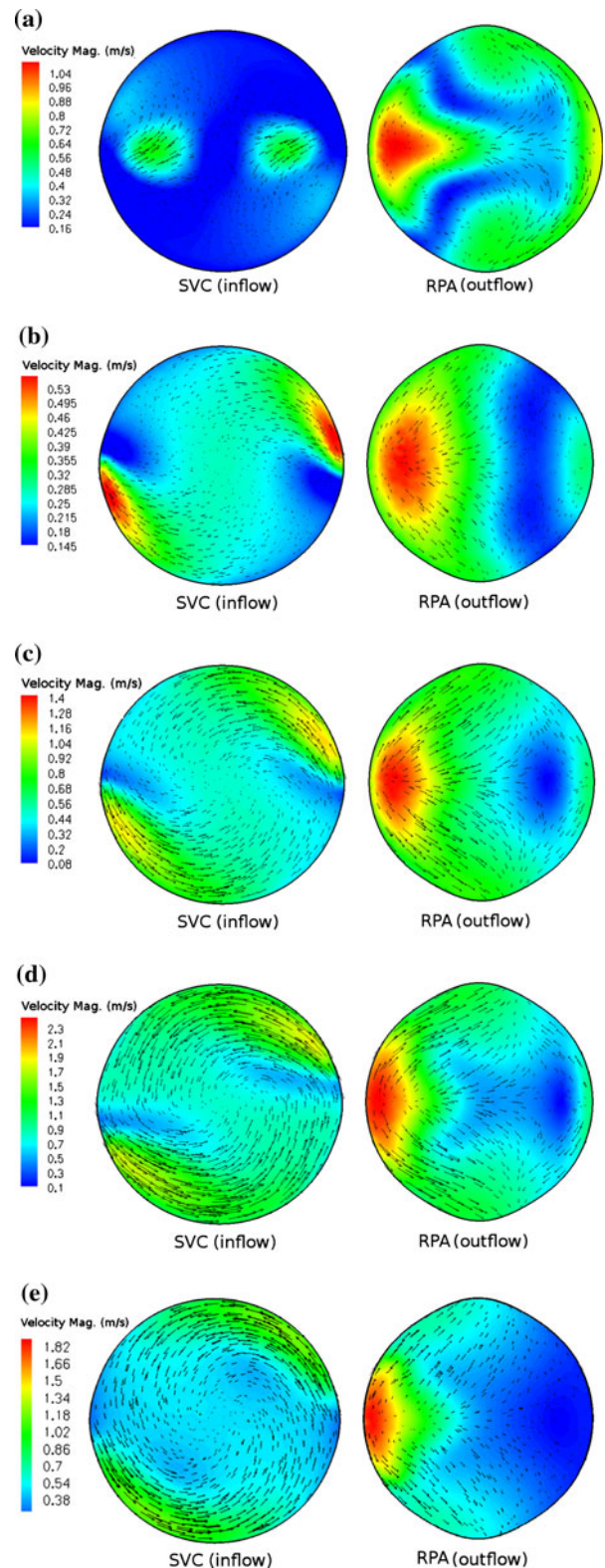


FIGURE 7. Flow patterns at 4.4 L/min. (a) Design 1: 2000 RPM. (b) Design 1: 3000 RPM. (c) Design 1: 4000 RPM. (d) Design 1: 5000 RPM. (e) Design 2: 5000 RPM.

and hemolysis testing. The VIP can perform in the target pressure rise over the desired range of flow rates with acceptable hemolysis potential.

In addition to right-sided circulatory support for late Fontan failure, a VIP may be applied to perioperative support after individual or combined Stage 2 or 3 palliative procedures under the existing staged protocol. This may shift the paradigm for treatment of Fontan patients, and solve many of the serious problems associated with the existing Fontan palliative strategy.

ACKNOWLEDGMENTS

We gratefully acknowledge partial financial support from the Indiana Clinical and Translational Sciences Institute, Indiana University and Purdue University. This work was also supported in part by National Institutes of Health grants HL080089 and HL098353.

REFERENCES

- ¹Anderson, J. B., H. G. Wood, P. E. Allaire, J. C. McDaniel, D. B. Olsen, and G. Bearnson. Numerical studies of blood shear and washing in a continuous flow ventricular assist device. *ASAIO J.* 46(1):486–494, 2000.
- ²Blackshear, P. L., and G. L. Blalock. Mechanical hemolysis. In: *Handbook of Bioengineering*, edited by R. Skalak and S. Chien. New York, NY: McGraw-Hill, 1987.
- ³Bludszuweit, C. Three-dimensional numerical prediction of stress loading of blood particles in a centrifugal pump. *Artif. Organs* 19(7):590–596, 1995.
- ⁴Dasi, L. P., K. Pekkan, H. D. Katajima, and A. P. Yoganathan. Functional analysis of fontan energy dissipation. *J. Biomech.* 41(10):2246–2252, 2008.
- ⁵Gillum, R. F. Epidemiology of congenital heart disease in the United States. *Am. Heart J.* 127:19–27, 1994.
- ⁶Giridharan, G. A., G. M. Pantalos, K. J. Gillars, S. C. Koenig, and M. Skliar. Physiologic control of rotary blood pumps: an in vitro study. *ASAIO* 50(5):403–409, 2004.
- ⁷Fluent Inc. *Fluent v6.3 User's Guide*, Lebanon, NH, 2006.
- ⁸Forstrom, R. J., and P. L. Blalock. Needles and hemolysis. *N. Engl. J. Med.* 283(4):208–209, 1970.
- ⁹Lacour-Gayet, F. G., C. J. Lanning, S. Stoica, R. Wang, B. A. Rech, S. Goldberg, and R. Shandas. An artificial right ventricle for failing fontan: in vitro and computational study. *Ann. Thorac. Surg.* 88(1):170–176, 2009.
- ¹⁰Litwak, K. N., S. C. Koenig, R. C. Cheng, G. A. Giridharan, K. J. Gillars, and G. M. Pantalos. Ascending aorta outflow graft location and pulsatile ventricular assist provide optimal hemodynamic support in an adult mock circulation. *Artif. Organs* 29(8):629–635, 2005.
- ¹¹Marsden, A. L., A. J. Bernstein, V. M. Reddy, S. C. Shadden, R. L. Spilker, F. P. Chan, C. A. Taylor, and J. A. Feinstein. Evaluation of a novel Y-shaped extracardiac Fontan baffle using computational fluid dynamics. *J. Thorac. Cardiovasc. Surg.* 137(2):394–403, 2009.
- ¹²Ohye, R. G., L. A. Sleeper, L. Mahony, J. W. Newburger, G. D. Pearson, M. Lu, C. S. Goldberg, S. Tabbutt, P. C. Frommelt, N. S. Ghanayem, *et al.* Comparison of shunt types in the norwood procedure for single-ventricle lesions. *N. Engl. J. Med.* 362(21):1980, 2010.
- ¹³Pantalos, G. M., S. C. Koenig, K. J. Gillars, G. A. Giridharan, and D. L. Ewert. Characterization of an adult mock circulation for testing cardiac support devices. *ASAIO* 50(1):1058–2916, 2004.
- ¹⁴Rodefeld, M. D., J. H. Boyd, B. J. LaLone, A. J. Bezrucko, A. W. Potter, and J. W. Brown. Cavopulmonary assist: circulatory support for the univentricular Fontan circulation. *Ann. Thorac. Surg.* 76:1911–1916, 2003.
- ¹⁵Rodefeld, M. D., B. Coats, T. Fisher, G. A. Giridharan, J. Chen, J. W. Brown, and S. H. Frankel. Cavopulmonary assist for the univentricular Fontan circulation: von Kármán viscous impeller pump. *J. Thorac. Cardiovasc. Surg.*, 140(3):529–536, 2010.
- ¹⁶Sobieski, M. A., G. A. Giridharan, M. Ising, M. S. Slaughter, and S. C. Koenig. Methodology of hemolysis testing of mechanical circulatory support devices. *ASAIO* 56:116, 2010.
- ¹⁷Soerensen, D. D., K. Pekkan, D. de Zlicourt, S. Sharma, K. Kanter, M. Fogel, and A. P. Yoganathan. Introduction of a new optimized total cavopulmonary connection. *Ann. Thorac. Surg.* 83:2182–2190, 2007.
- ¹⁸Svitek, R. G., D. E. Smith, and J. A. Magovern. In vitro evaluation of the TandemHeart pediatric centrifugal pump. *ASAIO* 53(6):747–753, 2007.
- ¹⁹Tamari, Y., K. Lee-Sensiba, E. F. Leonard, V. Parnell, and A. J. Tortolani. The effects of pressure and flow on hemolysis caused by Bio-Medicus centrifugal pumps and roller pumps. Guidelines for choosing a blood pump. *J. Thorac. Cardiovasc. Surg.* 106(6):997–1007, 1993.
- ²⁰Ungerleider, R. M., I. Shen, T. Yeh, Jr., J. Schultz, R. Butler, M. Silberbach, C. Giacomuzzi, E. Heller, L. Studenberg, B. Mejak, J. You, D. Farrel, S. McClure, and E. H. Austin. Routine mechanical ventricular assist following the Norwood procedure—improved neurologic outcome and excellent hospital survival. *Ann. Thorac. Surg.* 77(1):18–22, 2004.
- ²¹von Kármán, T. Über laminare und turbulente. *Z. Angew. Math. Mech.* 1:233–252, 1921.